J|A|C|S
ARTICLES
Published on Web 09/26/2002

Solid-State Ligand Dynamics in Interpenetrating $Mn[N(CN)_2]_2$(Pyrazine): A Neutron Spectroscopy Study

Craig M. Brown[†] and Jamie L. Manson*[,‡]

Contribution from the Materials Science Division, Argonne National Laboratory, 9700 South Cass Avenue, Building 200, Room A193, Argonne, Illinois 60439-4831, Department of Materials and Nuclear Engineering, University of Maryland, College Park, Maryland 20742, and NIST Center for Neutron Research, National Institute of Standards and Technology, Gaithersburg, Maryland 20899.

Received September 20, 2001. Revised Manuscript Received July 16, 2002

Abstract: We have used quasielastic neutron scattering to probe the solid-state ligand dynamics in the coordination polymer $Mn[N(CN)_2]_2$(pyz) {pyz = pyrazine} which has double-interpenetrating 3D lattices. A reversible structural phase transition occurs at 410 K as shown by neutron spectroscopy and differential scanning calorimetry. The origin of this transition is linked to rotational dynamics associated with the bridging pyz ligands. At 425 K, the pyrazine ring motion can be solely regarded as a 180° reorientational jump about the axis defined by the Mn−N coordinative bonds, occurring with a correlation time of ~70 ps. This model can be extended to the 200−410 K temperature region using high-resolution backscattering spectroscopy to measure an identical motion on the time scale of nanoseconds with an activation energy of 24 ± 2 kJ mol^{-1}. In contrast, no quasielastic scattering is seen for the 2D layered variant β-$Cu[N(CN)_2]_2$(pyz), owing to its more compact layer packing motif. Importantly, this work represents the very first study of solid-state rotational dynamics in an interpenetrating lattice structure.

Introduction

A theme in solid-state chemistry is the development of new molecular architectures with novel chemical and physical properties for applications such as chemical separation, catalysis, and magnetic devices. Compounds consisting of transition metal ions linked together by polydentate organic ligands are one class of materials, where the bonding motif and magnetic properties can be tuned over a wide range by varying either the transition metal or the ligands. The dicyanamide anion, $[N(CN)_2]^-$, is one such component that has been exploited to assemble supramolecular dia-, para-, antiferro-, and ferromagnetic materials.[1] The versatility of this anion arises from its variable coordinative behavior. For instance, $Zn[N(CN)_2]_2$ is a layered compound[1] with μ_2-bridging $[N(CN)_2]^-$, whereas the weakly ferromagnetic material $Mn[N(CN)_2]_2$ adopts a 3D rutile-type structure consisting of μ_3-$[N(CN)_2]^-$ bridges.[2] Further modifications may be obtained by introducing auxiliary π-conjugated ligands such as pyrazine (pyz), 4,4′-bipyridine, and 2,2′-bipyridine. These various molecular building blocks not only affect the spatial separation of the transition metal cations and the dimensionality of the crystal but also modulate the superexchange interactions. Other than the $M[N(CN)_2]_2$ {M = V, Cr, Mn, Fe, Co, Ni} compounds,[2,3] long-range magnetic ordering has been observed in a few other systems such as $Mn[N(CN)_2]_2$(pyz),[4,5] $Fe[N(CN)_2]_2$(pym)·S {pym = pyrimidine; S = pyrimidine, tetrahydrofuran, tetrahydropyran, ethanol, etc.},[6,7] and $Mn[N(CN)_2]_2(H_2O)_2$(2,5-me_2pyz$_2$).[8]

The structure of $Mn[N(CN)_2]_2$(pyz) can be described as an interpenetrating ReO_3-type network with axially elongated Mn^{2+} octahedra, where 2D $Mn[N(CN)_2]_2$ layers are connected via pyrazine ligands[4,5] (Figure 1a). Rietveld refinement of neutron powder diffraction (NPD) data at 1.35 K indicates a 3D antiferromagnetic ordering below T_N = 2.53(2) K, where the magnetic unit cell is doubled along the *a*- and *c*-axes relative to the monoclinic nuclear cell.[4] Substituting copper for manganese in this salt can result in a 2D layered β-$Cu[N(CN)_2]_2$(pyz) material that is weakly antiferromagnetic.[9] The crystal

[†] University of Maryland and National Institute of Standards and Technology.

[‡] Argonne National Laboratory. Telephone: (630) 252-6674. Fax: (630) 252-9151. E-mail: jlmanson@anl.gov.

(1) Manson, J. L.; Lee. D.-W.; Rheingold, A. L.; Miller, J. S. *Inorg. Chem.* **1998**, *37*, 5966.

(2) (a) Manson, J. L.; Kmety, C. R.; Epstein, A. J.; Miller, J. S. *Inorg. Chem.* **1999**, *38*, 2552. (b) Kmety, C. R.; Huang, Q.-z.; Lynn, J. W.; Erwin, R. W.; Manson, J. L.; McCall, S.; Crow, J. E.; Stevenson, K. L.; Miller, J. S.; Epstein, A. J. *Phys. Rev. B* **2000**, *62*, 5576. (c) Batten, S. R.; Jensen, P.; Kepert, C. J.; Kurmoo, M.; Moubaraki, B.; Murray, K. S.; Price, D. J. *J. Chem. Soc., Dalton Trans*. **1999**, 2987.

(3) (a) Manson, J. L.; Kmety, C. R.; Huang, Q.-z.; Lynn, J. W.; Bendele, G.; Pagola, S.; Stephens, P. W.; Epstein, A. J.; Miller, J. S. *Chem. Mater*. **1998**, *10*, 2552. (b) Batten, S. R.; Jensen, P.; Moubaraki, B.; Murray, K. S.; Robson, R. *Chem. Commun*. **1998**, 439. (c) Kurmoo, M.; Kepert, C. J. *New J. Chem*. **1998**, 1515.

(4) Manson, J. L.; Huang, Q.-z.; Lynn, J. W.; Koo, H.-J.; Whangbo, M.-H.; Bateman, R.; Otsuka, T.; Wada, N.; Argyriou, D. N.; Miller, J. S. *J. Am. Chem. Soc*. **2001**, *123*, 162.

(5) Manson, J. L.; Incarvito, C. D.; Rheingold, A. L.; Miller, J. S. *J. Chem. Soc., Dalton Trans*. **1998**, 3705.

(6) Manson, J. L. Unpublished results.

(7) Kusaka, T.; Ishida, T.; Hashizume, D.; Iwasaki, F.; Nogami, T. *Chem. Lett*. **2000**, 1146.

(8) Manson, J. L.; Schlueter, J. A.; Geiser, U.; Stone, M. B.; Reich, D. H. *Polyhedron* **2001**, *20*, 1423.

(9) (a) Manson, J. L. Unpublished results. (b) Jensen, P.; Batten, S. R.; Fallon, G. D.; Hockless, D. C. R.; Moubaraki, B.; Murray, K. S.; Robson, R. *J. Solid State Chem*. **1999**, *145*, 387.

10.1021/ja017124b CCC: $22.00

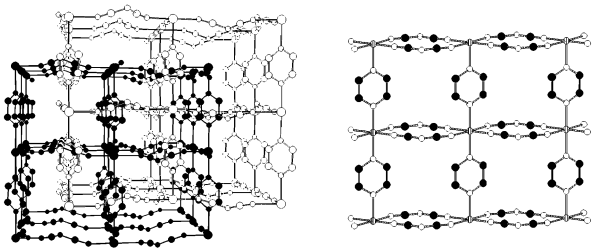

Figure 1. (a) Crystal structure of 3D ReO_3-type Mn[N(CN)$_2$]$_2$(pyz) showing the two interpenetrating lattices. (b) Crystal structure of 2D β-Cu[N(CN)$_2$]$_2$-(pyz). Hydrogen atoms have been omitted for clarity.

structure consists of octahedrally coordinated Cu^{2+} ions with 1D Cu[N(CN)$_2$]$_2$ ribbons cross-linked by pyz ligands (Figure 1b). In the current article, we report a quasielastic neutron scattering study of the solid-state ligand dynamics in these systems. Quasielastic scattering involves the Doppler-like broadening of scattered neutrons due to reorientational or diffusive motions of atoms in the probed material.

The neutron has several properties that make neutron scattering a particularly valuable technique for probing the dynamics of materials. Neutrons that have wavelengths on the order of interatomic spacing also possess energies on the same order as those characteristic of phonon and intermolecular interactions. This provides a mechanism to measure both structural and temporal information, simultaneously. The interaction may also be isotope dependent being particularly important for hydrogen and deuterium. Finally, the neutron has a magnetic moment, which interacts with unpaired electrons, allowing magnetic systems to be investigated.

Experimental Section

Nondeuterated ("protonated") β-Cu[N(CN)$_2$]$_2$(pyz) and Mn[N(CN)$_2$]$_2$-(pyz) were synthesized as reported previously,[4,5,9] while the deuterated sample was the same one used to elucidate the magnetic structure.[4] Thermal analyses were performed on either a TA Instruments Model 2910 or Perkin-Elmer Pyris 1 differential scanning calorimeter (DSC) and a TA Instruments Model 2050 thermal gravimetric analyzer (TGA). Temperature control was maintained between 120 and 770 K and between ambient and 1270 K for the DSC and TGA instruments, respectively. All samples were weighed using the TGA balance ($\pm$10 μg) with sample sizes ranging from 1.5 to 2.5 mg. DSC samples were weighed and hermetically sealed in aluminum pans. A heating rate of 10 K min^{-1} was utilized for all DSC and TGA experiments.

Quasielastic neutron scattering measurements on Mn[N(CN)$_2$]$_2$(pyz), the deuterated analogue, and β-Cu[N(CN)$_2$]$_2$(pyz) were performed with the Fermi-chopper spectrometer (FCS)[10] and the high flux backscattering spectrometer (HFBS)[11] at the NIST Center for Neutron Research. The approximately 5-g samples were placed inside identical annular aluminum sample holders and press-sealed with lead wire. The annular geometry was chosen to keep the scattering probability to $\sim$0.1. Temperature control was achieved using a modified closed-cycle helium refrigerator that could heat the sample to 480 K.

FCS is a direct-geometry time-of-flight instrument. For measurements of the quasielastic scattering, a neutron wavelength of 6.0 Å was used, resulting in an instrumental resolution of $\sim$65 μeV at the elastic line. Spectra were collected at 330, 390, and 425 K for both the nondeuterated and deuterated manganese samples with data collection times of approximately 24 h. The measurement of the deuterated manganese was performed in order to subtract contributions to the protonated data from paramagnetic scattering. Additional information on the low energy generalized phonon density of states, $G(\omega)$, was collected using an incident neutron wavelength of 4.8 Å in neutron energy gain. The poorer elastic resolution at this wavelength ($\sim$0.145 meV) is compensated for by the increase in available momentum transfer and a more complete averaging over the Brillouin zone for the resulting $G(\omega)$. For all samples, the generalized phonon densities of states data (4.8 Å) were collected at 150, 300, and 425 K. An empty aluminum container data set taken at either 200 or 400 K was used to correct for the instrumental background. The data were reduced using standard programs, and $G(\omega)$ was estimated self-consistently with multiphonon expansion up to the sixth term taken into account using the program Muphocor.[12]

HFBS is a high-energy resolution backscattering spectrometer in which Doppler shifting of the neutrons about a normal incident wavelength of 6.271 Å varies the incident neutron energy. The crystal analyzer system allows only neutrons with a fixed final energy to reach the detectors. Measurements were performed on the nondeuterated Mn-[N(CN)$_2$]$_2$(pyz) and the related β-Cu[N(CN)$_2$]$_2$(pyz) system. The sample was placed in a $\sim$1-mm thick pouch made from aluminum foil, which was then wedged into a cylindrical aluminum can (diameter 3 cm, length 3 cm) and mounted in a closed cycle refrigerator which had been modified for high temperature operation. Initially, the sample was cooled to 100 K, and a *stationary* Doppler scan (fixed window scan) was performed. The sample temperature was ramped at 0.4 K min^{-1}, with data recorded every 2 min, to 435 K. For a purely harmonic, incoherent scattering system, the intensity of the elastic line follows a Q-dependence determined by the Debye−Waller factor

$$I(Q) = I_0 e^{-Q^2u^2} \tag{1}$$

The difference between the u^2 at a given temperature and the base temperature, T_B, can be obtained simply by normalizing the measured intensities to those measured at T_B (where the scattering is primarily elastic). In a plot of Δu^2 versus temperature, any nonlinear behavior can be attributed to the presence of increasing quasielastic scattering moving elastic intensity outside of the resolution window. Additional "Doppler scans", with an energy transfer window of $\pm$37 μeV and an energy resolution of $\sim$1 μeV, recorded $S(Q, \omega)$ from 200 to 425 K with 25-K intervals and data collection times between 10 and 20 h. Only the nondeuterated manganese complex was studied on HFBS because the time scale of the paramagnetic scattering is too fast to be observed on this instrument. There was no evidence of additional dynamics in the β-Cu complex.

Analysis of quasielastic scattering data, in a well-defined system, is very much simplified by employing a strong incoherent scatterer, such as hydrogen. This eliminates the need to model pairwise interactions between atoms and concentrates solely on the dynamics of the individual hydrogen atoms. For an incoherent scatterer undergoing reorientational motion, the scattering law may be written as

$$S^{inc} = [A_0(Q)\delta(\omega) + \sum_{i=1}^{n} A_i(Q)L_i(Q,\omega,\Gamma_i)]\, e^{-Q^2U^2} \otimes R(\omega) \tag{2}$$

For quasielastic fitting, we employed a single delta-function at zero energy transfer, of integrated area A_0, in combination with a broader Lorentzian peak, L_1, of integrated area A_1 and width Γ_1, both convoluted with the resolution function, $R(\omega)$ appropriate for the instrument, at each momentum transfer. A measure of the quasielastic scattering is embodied in the "elastic incoherent structure factor", EISF, the ratio of the elastic scattering to the total scattered intensity. From the Q-dependence of the EISF,[13,14] it is possible to deduce information about the geometry of single particle hydrogen motion, while the width of

(10) Copley, J. R. D.; Udovic, T. J. *J. Res. Natl. Inst. Stand. Technol.* **1993**, *98*, 71.
(11) Gehring, P. M.; Neumann, D. A. *Physica B* **1998**, *241−243*, 64.
(12) Reichardt, W. *Muphocor*; Kernforschungszentrum Karlsruhe, 1984.
(13) Bée, M. *Quasielastic Neutron Scattering*; Adam Hilger: Bristol, 1988.
(14) Yildirim, T.; Gehring, P. M.; Neumann, D. A.; Eaton, P. E.; Emrick, T. *Phys. Rev. B* **1999**, *60*, 314.

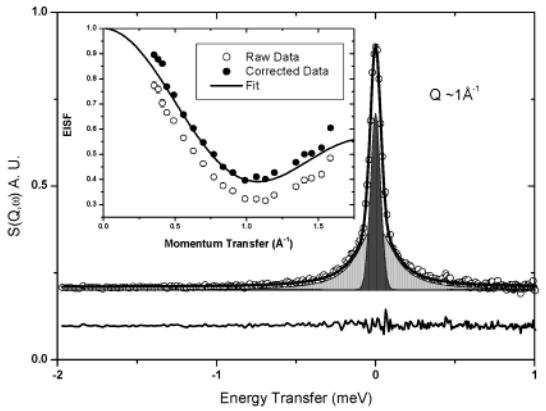

Figure 2. Quasielastic spectrum at 425 K of $Mn[N(CN)_2]_2(pyz)$ at a momentum transfer of ~1 Å^{-1} (open circles) is fitted to an elastic delta-function (dark gray solid) and a broader Lorentzian component (light gray solid) both convoluted with the instrumental resolution. The fit and difference curves are also shown as a line through the data and beneath, respectively. The insert shows the EISF for the protonated complex (open circles). After subtracting the measured contribution from paramagnetic scattering, one obtains the scattering due entirely to hydrogen (solid circles). The solid line depicts a fit to the 2-fold jump model with only one adjustable parameter.

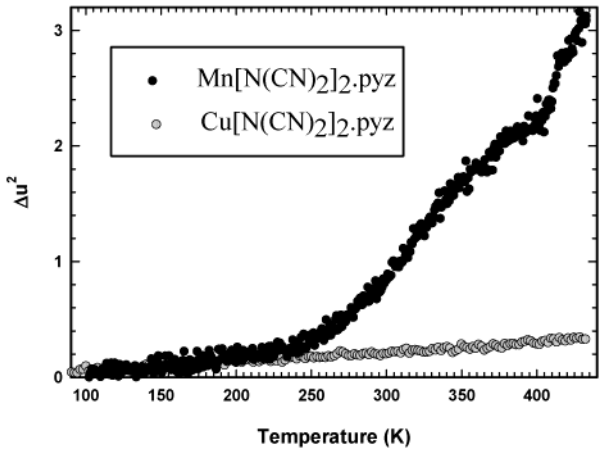

Figure 3. Variation of the effective mean-square displacement with temperature from the elastic-scan technique. Data for $Mn[N(CN)_2]_2(pyz)$ are shown as black filled circles with comparable data taken on the β-Cu-$[N(CN)_2]_2(pyz)$ salt shown as gray circles. The first increase of the curve at ~250 K is due to the gradual onset of rotational pyrazine motion. The sharp increase at ~410 K coincides with another transition, where all pyrazines are performing a much faster 2-fold jump reorientation.

the quasielastic peak gives information about the time scale of the motion. Since we are only interested in incoherent scattering for the EISF, all detectors that have contributions from coherent scattering such as Bragg peaks were excluded from the fits.

Results and Discussion

Thermal Analyses. The results of the TG and DSC measurements on $Mn[N(CN)_2]_2(pyz)$ are described. A single sharp weight loss of 29.89% occurs between 433 and 533 K, consistent with the loss of one pyrazine molecule per formula unit (29.98% calculated). Above 533 K, only a gradual weight loss is observed to a maximum temperature of 775 K. DSC experiments display endothermic processes at ~408 and ~511 K. Interestingly, the thermal event occurring at 408 K is not due to weight loss according to the TG trace and, therefore, is almost certainly the result of a structural phase transition. Continual heating above 533 K results in a gradual decomposition of the sample. From DSC, the β-$Cu[N(CN)_2]_2(pyz)$ sample decomposes near 525 K.

Time-of-Flight Neutron Scattering. The QENS spectra obtained on FCS clearly show the effect of the phase transition. At 425 K, the quasielastic signal in the protonated pyrazine compound is significantly larger than that in the deuterated complex, whereas, for temperatures below 408 K, the small quasielastic signal we observe is similar to those in the protonated and deuterated materials, because of the presence of paramagnetic Mn^{2+} ions and possible weaker coherent contributions arising from dynamics in the dicyanamide ligand and deuterium. In Figure 2, we show a fit to a typical $S(Q,\omega)$ spectrum at 425 K along with the decomposition into a Gaussian elastic peak and a broad Lorentzian. Attempts to decompose the quasielastic scattering into two independent Lorentzian components, one of which represents the paramagnetic scattering, were not successful. We have estimated the quasielastic scattering due to paramagnetism and the coherent scattering from the nonproton ligands as the integrated quasielastic intensity observed in deuterated $Mn[N(CN)_2]_2(pyz)$. The inset of Figure 2 shows the Q-dependence of the EISF for the protonated compound and the same data after subtracting the quasielastic scattering obtained from the deuterated compound. This approach is justified in that the incoherent scattering of the deuteron is very small. Nevertheless, this increases the EISF by ~0.07 at all momentum transfer values. The EISF displays a minimum at a distinct inverse length scale and a high Q value that tends toward one-half. These features are consistent with a 2-fold jump model[13−15]

$$\mathrm{EISF} = \frac{1}{2}\left(1 + \frac{\sin(Qr)}{(Qr)}\right) \qquad (3)$$

where the only variable parameter is the proton jump distance, r. The solid line in Figure 2 is a fit to the corrected data, resulting in a proton−proton jump distance of 4.17(1) Å.[16] Rietveld refinement of neutron powder diffraction data[4] gives the average D−D distance across the pyrazine ring as 4.16(2) Å at 2.5 K. Thus, the pyrazine ligands perform novel 2-fold jumps about the axis defined by the coordinating nitrogen atoms. Further, the width of the quasielastic peak is approximately constant over the entire Q-range, as is expected for this type of motion. The correlation time, τ, for the π-jumps, given by $\Gamma_1/4$, is 70(1) ps at 425 K.

Neutron Backscattering Spectroscopy. Figure 3 shows the mean squared displacement values as a function of temperature for $Mn[N(CN)_2]_2(pyz)$ and β-$Cu[N(CN)_2]_2(pyz)$ extracted from the fixed window scans over a momentum transfer range of 0.2−1.2 Å^{-1}. While the data for β-Cu are linear over the entire temperature range studied, there is an increase in Δu^2 for the manganese sample between 200 and 250 K followed by a step at ~410 K. While there are similarities between these temperatures and the phase transitions observed by diffraction[17] and DSC for the manganese complex, Δu^2 only reflects the temperature dependence of the quasielastic spectrum with respect to the width of the resolution window. Data taken on cooling from 435 K show an identical dependence of Δu^2 with

(15) Dianoux, A. J.; Volino, F.; Hervet, H. *Mol. Phys.* **1975**, *30*, 1181.
(16) While the fit is excellent, there is a tendency for the data to be shifted slightly above the fitted curve at higher Q values. This would be the case if a small amount of extra coherent scattering, possibly originating from coherent diffuse scattering, was present over this range.
(17) (a) Brown C. M. et al. To be published. (b) Jensen, P.; Batten, S. R.; Moubaraki, B.; Murray, K. S. *J. Solid State Chem.* **2001**, *159*, 352.

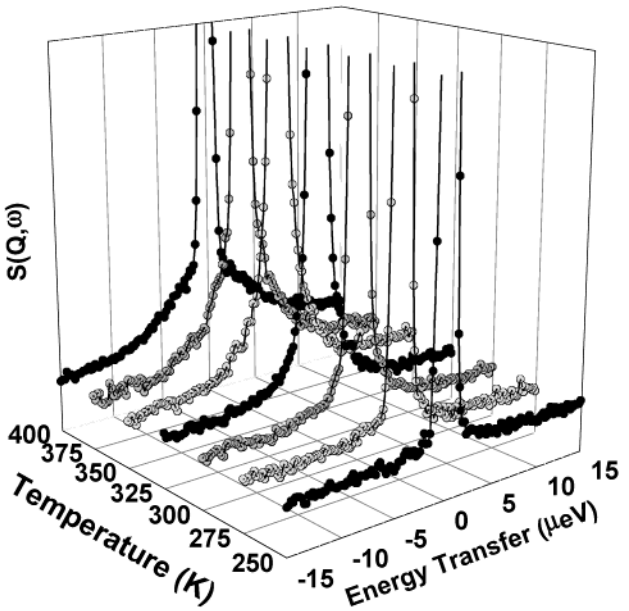

Figure 4. Temperature dependence of the scattering law for $Mn[N(CN)_2]_2$(pyz), summed over detectors, to emphasize the growth of the quasielastic scattering on HFBS. There is an increase in intensity of the quasielastic component as the temperature is raised to 400 K.

temperature, indicating that the phase transitions are reversible within the resolution of the instrument. Figure 4 displays *Q*-integrated energy scans for $Mn[N(CN)_2]_2$(pyz) obtained every 25 K between 250 and 400 K. While this plot does not convey the *Q*-dependence of the scattering, it does illustrate that the quasielastic intensity increases with temperature.

Fitting the *Q*-resolved data to the model given by eq 2 and obtaining a smoothly varying EISF is somewhat difficult because of the rather poor *Q*-resolution on HFBS and data statistics. The main problem is that most of the detectors have some contribution from coherent Bragg scattering for this large, low symmetry unit cell. Having carefully investigated various fitting procedures and removing those detectors contaminated most by Bragg scattering, we find that the EISF is very similar to that obtained at 425 K on the FCS spectrometer, with an additional elastic component. To account for this extra elastic component, we added an extra parameter to the fit of the EISF that can be interpreted as a fraction of the total number of hydrogens that are stationary. Also, since the number of data points are limited, we constrained the jump distance to be that deduced from the 425-K FCS data, so allowing the data to be fitted with only one parameter, the fraction of hydrogen atoms performing 2-fold jumps, *f*. Figure 5 shows that *f* exhibits an almost sigmoidal increase with temperature with the inset detailing selected EISF data and fits. However, even at 400 K, the entire sample does not appear to be performing the 180° jump motion. It is possible that even though most Bragg contaminated detectors have been removed from this fitting procedure, the remaining detectors do have some coherent contributions that tend to increase the value of the EISF. An explanation of this temperature dependence could be the existence of a correlated motion of the ring flips with the dynamics of the dicyanamide ligand. For low temperatures, there are many pyrazines that are in close proximity to the framework structure, resulting in a low probability of a rotational jump. Presumably, as the temperature increases, the lattice expansion and larger amplitude librations/vibrations of the dicyanamide ligand can combine to reduce

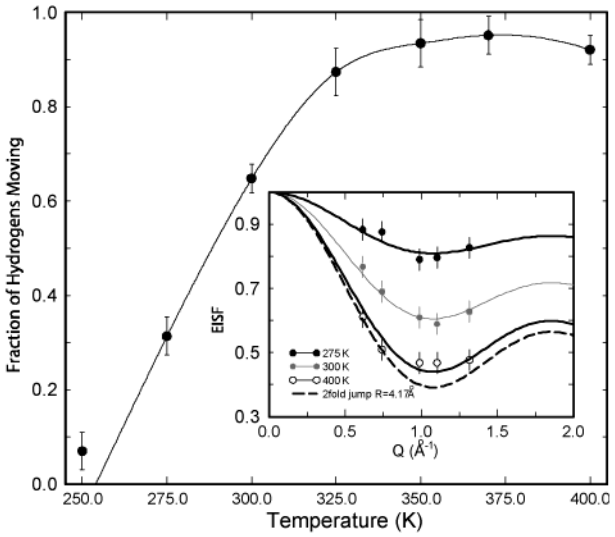

Figure 5. Evolution of the fraction of hydrogens jumping, *f*, as a function of temperature; the solid line is a guide to the eye. The inset shows the EISF and fits to the 2-fold jump model at three temperatures.

the rotational potential barrier for an increasing fraction of the pyrazines. As yet, we are unable to offer a proof why the pyrazine fraction behaves in this manner or if there exists a motion on a much slower time scale.

We can have more confidence in the extracted quasielastic line widths compared to the EISF for the backscattering data, as this is essentially independent of the elastic scattering and can be fitted for all available detectors. The correlation times obtained from the line widths for the 180° jump motion changes from ~17 nanoseconds to 1.9 ± 1 nanoseconds upon increasing the temperature from 250 to 400 K. The abrupt increase in τ from 1.9 to 70 ps between 400 and 425 K coincides with the phase transition at 408 K. The activation energy, E_a, for the jump process between 250 and 400 K is 24 ± 2 kJ mol^{-1}.

This type of motion has been reported on substantially longer time scales for similar large organic fragments in purely molecular solids on the basis of the analysis of solid-state NMR line shapes. Examples include phenylene ring flips in poly(*p*-phenylene vinylene) films ($E_a = 63$ kJ mol^{-1}),[18] phenyl ring flips of various ligands in crystalline carboxypeptidase,[19] and rotational jumps of *p*-diiodobenzene about the 1−4 axis ($E_a = 90$ kJ mol^{-1}).[20] The correlation times are consistently on the order of microseconds. Within the time scale window available to neutron quasielastic scattering, 180° rotational jumps are rarely observed. Documented cases include the rotational motion of small anions such as hydrogensulfides[21] and the NH_2 unit in monoclinic potassium amide with a large activation energy of 185 meV and a correlation time of 33 ps at 324 K.[22] Two-fold jumps about a 4-fold axis have been observed in the much larger molecular system of cubane, whose orientational potential is mainly determined by van der Waals interactions.[14] In the present case, the relatively large volume available to each

(18) Simpson, J. H.; Rice, D. M.; Karasz, F. E. *J. Polymer Sci., Part B: Polym. Phys.* **1992**, *30*, 11.
(19) Zhang, H.; Bryant, R. G. *Biophys. J.* **1997**, *72*, 363.
(20) Aliev, A. E.; Harris, K. D. M.; Alcobe, X.; Estop, E. *J. Chem. Soc., Faraday Trans.* **1993**, *89*, 3797.
(21) Haarmann, F.; Jacobs, H.; Asmussen, B.; Noldeke, C.; Kearley, G. J.; Combet, J. *J. Chem. Phys.* **2000**, *113*, 8161.
(22) Müller, M.; Asmussen, B.; Press, W.; Senker, J.; Jacobs, H.; Büttner, H.; Schober, H. *J. Chem. Phys.* **1998**, *109*, 3559.

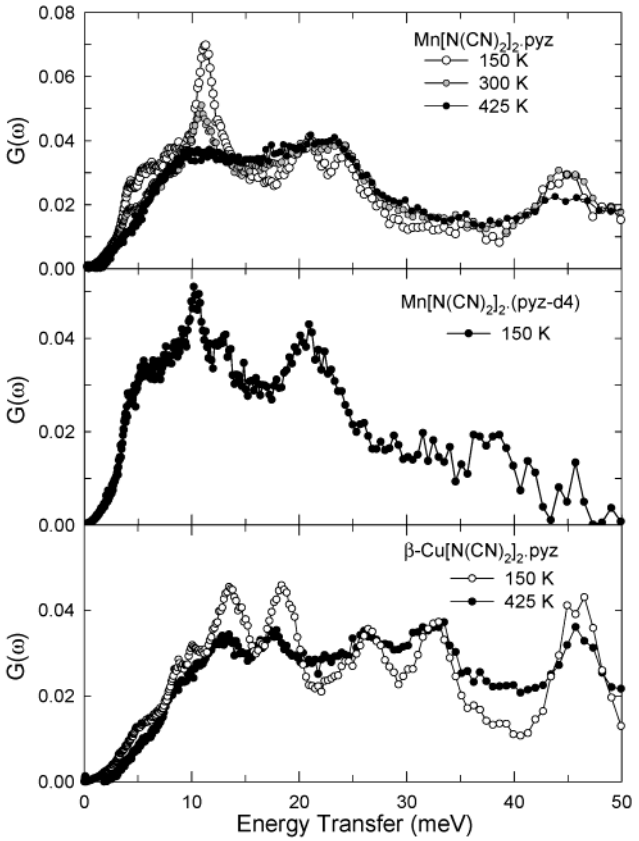

Figure 6. (Upper) Phonon densities of states, in neutron energy gain, of $Mn[N(CN)_2]_2(pyz)$ at 150, 300, and 425 K are shown as white, gray, and black circles, respectively. (Middle) $G(\omega)$ values for the deuterated $Mn[N(CN)_2]_2(pyz)$ complex at 150 K. (Bottom) $G(\omega)$ values for the β-$Cu[N(CN)_2]_2(pyz)$ complex at 150 and 425 K.

pyrazine in the interpenetrating lattice is sufficient to result in a low rotational barrier, allowing these large molecular fragments to rotate on the unusually short time scales observed here.

Phonon Densities of States. The phonon densities of states for $Mn[N(CN)_2]_2(pyz)$ are shown at three temperatures in the upper panel of Figure 6. In neutron energy gain, the resolution worsens considerably with increasing energy transfer, being 2.4 meV at a transfer of 20 meV. In addition to the general broadening and softening of the spectral features with temperature, the intense peak at ~11.2 meV is strongly attenuated on passing to the highest temperatures, where we observe the fastest pyrazine dynamics. $G(\omega)$ for the deuterated sample at 150 K is shown in the middle panel of Figure 6. All of the three main features at ~10, 24, and 45 meV show isotopic shifts. In particular, the feature at 10.4 meV has softened from an equivalent 11.2 meV in the protonated sample, consistent with the isotopic shift expected for a librational mode of the pyrazine ring about the N−N axis. Moreover, the intensity of this peak rapidly decreases with increasing temperature, as expected for this libration on the basis of the quasielastic results. Assuming that the 2-fold potential for the pyrazine libration potential can be well-represented by the first term in a Fourier expansion, one easily obtains a relation between the librational frequency, $\hbar\omega$, the moment of inertia, I, and the librational activation energy, V_B

$$\hbar\omega = 2\sqrt{\frac{\hbar^2}{2I}V_B} \qquad (4)$$

Using the moment of inertia from the low temperature neutron structure, the activation energy is calculated to be 115 kJ mol^{-1}. This activation energy is much larger than that at the experimental temperature where one observes fully dynamic pyrazines (425 K is equivalent to 3.5 kJ mol^{-1}) and is about 5 times larger than the activation energy derived from the backscattering data. These incompatibilities probably reflect a significant change in V_B at the high temperature phase transition and a much more complicated energy landscape at the low temperatures than assumed from a simple cosine potential.

For comparison, we show $G(\omega)$ values for β-$Cu[N(CN)_2]_2(pyz)$ at 150 and 425 K in the bottom panel of Figure 6. The retention of the main peaks with increasing temperature agrees with the absence of any phase change and the lack of reorientational motions of the pyrazines within this layered structure. The high frequencies of these peaks imply a larger barrier to rotation for the pyrazine rings compared to that for the manganese material. Comparing the local pyrazine environments in the manganese and copper crystal structures indicates that the volume available for the pyrazine is smaller in the copper complex. Consider the pyrazine protons of closest proximity to the framework as a function of the rotation angle about the N−N axis. The closest distance for a proton to any atom in the dicyanamide ligands is ~1.95 Å for $Mn[N(CN)_2]_2(pyz)$ and ~1.7 Å for β-$Cu[N(CN)_2]_2(pyz)$ at similar temperatures of ~175 K. In both cases, the shortest contact is between a proton and the amide N atom. Preliminary analysis of neutron diffraction data taken at 250 K indicates that this distance only moderately increases to ~2.0 Å, evidently a large enough increase to facilitate the observed 2-fold jump motion that we observe at this temperature.

Density functional theory (DFT) calculations performed on chemically simplified molecular fragments of the lattice allow one to pinpoint the origins of essentially molecular modes. We used the Gaussian98 package[23] to calculate the normal modes of free $[Mg-pyz-Mg]^{4+}$ and $[Mg-NCNCN-Mg]^{-}$ fragments using the $Mn[N(CN)_2]_2(pyz)$ crystallographic data. Magnesium ions were chosen to replace Mn^{2+} in order to remove difficulties associated with an open-shell spin configuration and to further simplify the calculations. Geometry optimization and vibrational frequency calculations were performed using the Becke three-parameter hybrid functional[24] with the Lee−Yang−Parr correlation function[25,26] and 6-311G basis sets[27,28] for all atoms. From comparison of these calculations and neutron vibrational spectroscopy data, we are confident that this limited use of the DFT formalism can yield reasonable descriptions of the eigenvalues and eigenvectors for these normal modes. These results indicate that the mode at ~20 meV in $Mn[N(CN)_2]_2(pyz)$ is a rocking of the pyrazine ring about the axis defined through both C═C bonds of the ring. The higher energy mode at ~46 meV is a ring torsion of a symmetry that is slightly shifted in frequency from the 43 meV observed in the pure pyrazine solid and calculated at both Hartree−Fock and MP levels of theory.[29]

(23) Frisch, M. J. et al. *Gaussian 98*, revision A.7; Gaussian, Inc.: Pittsburgh, PA, 1998.
(24) Becke, A. D. *J. Chem. Phys.* **1993**, *98*, 5648.
(25) Lee, C.; Yang, W.; Parr, R. G. *Phys. Rev. B* **1988**, *37*, 785.
(26) Vosko, S. H.; Wilk, L.; Nusair, M. *Can. J. Phys.* **1980**, *58*, 1200.
(27) McLean, A. D.; Chandler, G. S. *J. Chem. Phys.* **1980**, *72*, 5639.
(28) Krishnan, R.; Binkley, J. S.; Seeger, R.; Pople, J. A. *J. Chem. Phys.* **1980**, *72*, 650.
(29) Kearley, G. J.; Tomkinson, J.; Navarro, A.; López-González, J. J.; Fernández-Gómez, M. *Chem. Phys.* **1997**, *323*−*335*, 216.

The corresponding low energy mode for β-$Cu[N(CN)_2]_2$(pyz) could have softened slightly to below 20 meV, while the higher mode at 45 meV is in good agreement.

Conclusions

We have shown that $Mn[N(CN)_2]_2$(pyz) exhibits a phase transition at 408 K. The pyrazine ligand is seen to librate in a deep potential in the low temperature monoclinic phase. At about 200 K, a thermally activated 2-fold jump motion about the coordinating nitrogen axis takes place. As the temperature is increased toward 400 K, the fraction of pyrazine rings performing this motion increases with a slight increase in the correlation time of the jump, increasing from 1.9 to 17 ns. The activation energy for this process is 24 ± 2 kJ mol^{-1}. The phase transition at 408 K, evidently, results in a much more open framework structure as the correlation time for the 2-fold jump increases to 70 ps, an unusually short time for a molecular fragment this size. By comparison, the β-$Cu[N(CN)_2]_2$(pyz) analogue has a more compact 2D layer packing that restricts pyrazine rotational dynamics at any temperature studied on the nanosecond to picosecond time scales.

Acknowledgment. C.M.B. gratefully acknowledges the support received from the NCNR during this project and especially Dan Neumann for his advice and critical reading of this manuscript. J.L.M. thanks G. Wiederrecht for access to the thermal analyses equipment at Argonne National Laboratory. The Office of Basic Energy Sciences, Division of Materials Science, U.S. Department of Energy under contract W-31-109-ENG-38 supported work performed at Argonne National Laboratory. Identification of commercial equipment in the text is not intended to imply any recommendation or endorsement by the National Institute of Standards and Technology.

JA017124B